LOW FREQUENCY EDDY CURRENT ARRAYS WITH VIDEO CLOCK

Gerhard MOOK, Fritz MICHEL, Jouri SIMONIN
Otto-von-Guericke-University Magdeburg, Germany

Peter ROST
BASF SE Ludwigshafen, Germany

1. Introduction

Eddy current arrays are able to visualize the inspected area avoiding complicated impedance plane diagrams [1-20]. Fig. 1 shows bimodal sensors arranged to an array. The point spread function (PSF) of every sensor element differs significantly. The pitch-catch probe shown in the left column of Fig. 1 is based on one central transmitting coil and six receiving neighbouring coils. The number of probes formed by this method is more than twice the number of coils. The single core probe in the right column of Fig. 1 spreads its magnetic field also to all neighbours but is recorded by the transmitting element. The number of probes equals the number of cores. This way, two operation modes may be used: the pitch-catch mode and the single core mode. In any mode a transmitter selector switches the transmitting coils and a receiver multiplexer switches the receiver coils. Both work independently each from other. In any time slot only one probe is active.
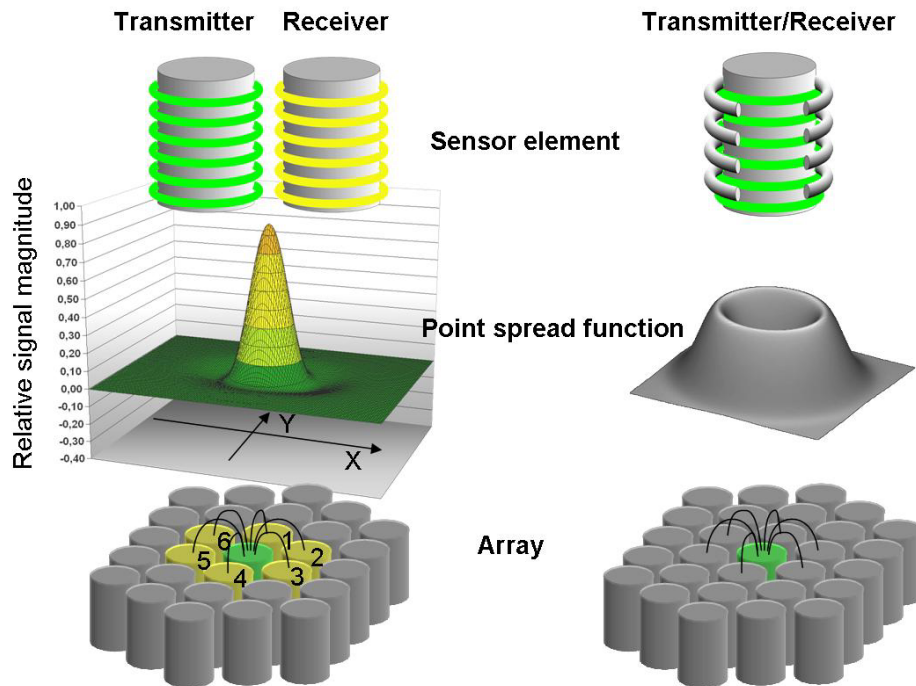

Fig. 1: Bimodal sensors, their point spread function and cascading to an array.
Left: Pitch-catch probe, right: single core probe (parametric or transformer)

Concerning the quality of imaging, the spatial resolution plays an important role. In the single core mode every coil corresponds to one probe, the spatial resolution is that of the core density. Along a probe line the PSFs are superimposing like shown in Fig. 2 above. The part below explains, that in the pitch-catch mode the spatial resolution along a probe line is twice as high.
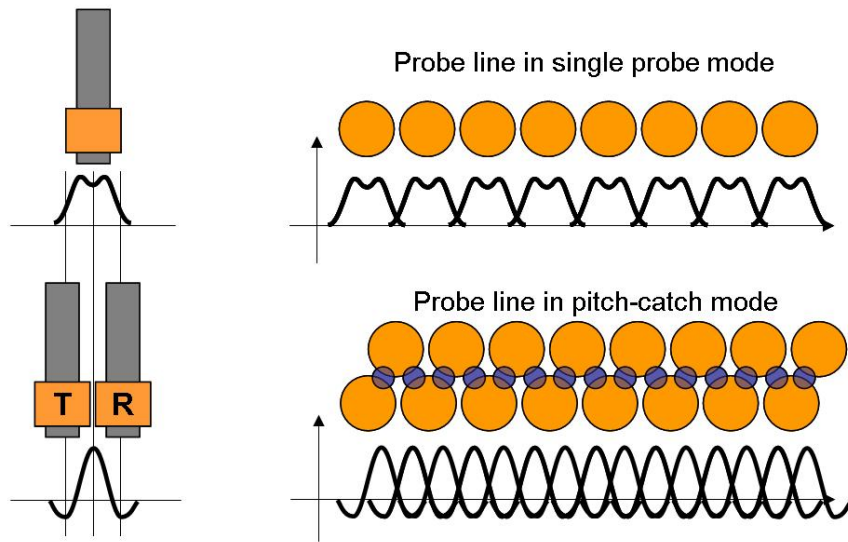
Fig. 2: Spatial resolution in single mode (above) and pitch-catch mode (below)

2   Sensor elements

The pitch-catch probe type offers the opportunity of increasing inspection depth [21, 22]. Fig. 3 brings up the principle of these probes. The magnetic field of the exciting coil penetrates accordingly to the well known rules of alternating field spreading into the material. The receiving coil only picks up this part of the flux, which has penetrated deeply into the material. The larger the spacing between the two coils the deeper the detected flux lines have penetrated into the material but the lower becomes the measurement signal.

This system of two non-axial coils may be considered as an axial coil system with a diameter corresponding to the coil distance of the non-axial system. With increasing distance (or diameter) of the coils the defect volume decreases relatively to the volume of interaction lowering the signal amplitude. One has to trade off between these parameters.
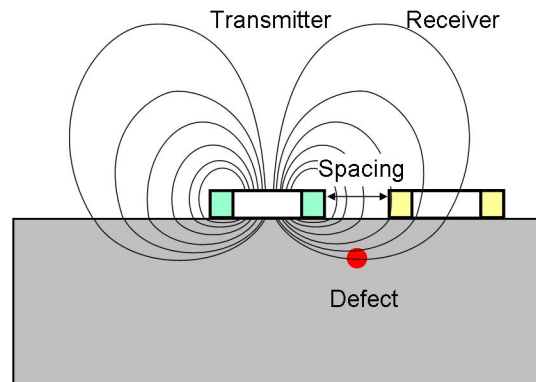

Fig. 3: Non-axial probe selects deep penetration field trajectories

For assessing the chances for defect characterization the complex values of the measurement voltage were calculated for different inspection situations. Commonly all defect signals are referred to the lift-off signal. For calculating the VIC-3D® code was used.

Fig. 4 brings up the signal behaviour of a pore with defined underlying. On sound material the signal is centred at the balance point. When approximating a defect the signal trajectory starts with negative y-values. Just like axial probes the signal turns to positive y-values over the defect. The defect signal turns clockwise with increasing defect underlying. This circumstance opens up the opportunity of assessing the defect underlying. The signal magnitude mirrors the defect volume.
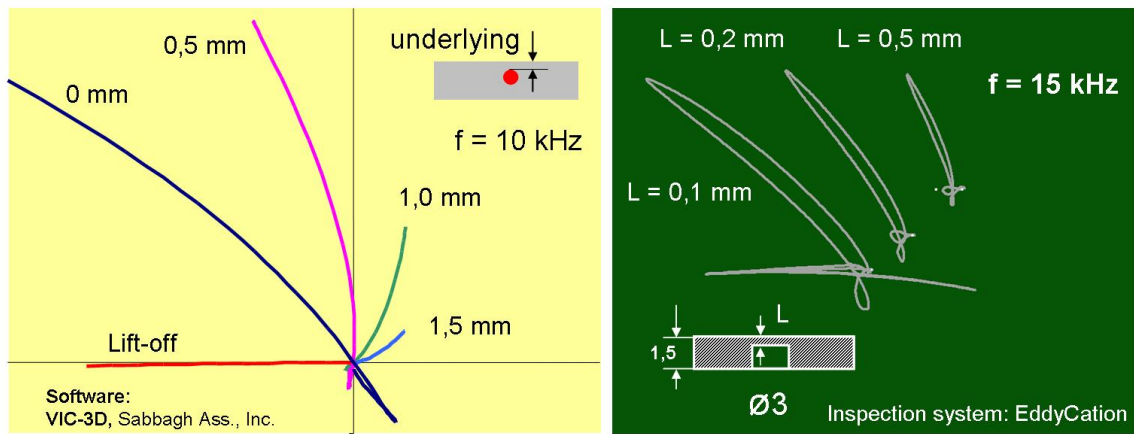
Fig. 4: Complex measurement signal of a pitch-catch-probe moving over hidden pores.
Left: calculated signals, right: measured signals.

3 Flat sensor lines

Two sensor lines have been manufactured each consisting of 32 and 64 rod core coils respectively. The speed of electronic field movement ranges from 0.3 to 3 m/s according to the inspection requirements. To visualize a certain area of the workpiece the sensor line must be guided over the surface. When handled manually a measuring wheel connected to the sensor picks up the distance. In automatic inspection a robot can guide the sensor with constant velocity from 6 to 48 mm/s. Fig. 5 displays the sensor lines. The eddy current instrument is reduced to a multiplexer and an AD/DA-converter. All necessary electronics is placed in the probe housing. A simple USB cable connects the probe line to a notebook. All other components and functions are addressed to the software.

Fig. 5: Left: Array probe 32, 1.5-mm-ferrite rod cores, pitch-catch mode, coil centre distance 3 mm, total track width 45 mm, probe centre distance 1.5 mm,
right: Array probe 64, 1.05-mm-ferrite rod cores, pitch-catch mode, coil centre distance 2 mm, total track width 61 mm, probe centre distance ca. 1 mm

For the assessment of the probe lines an aluminium sheet was engraved with letters and signs simulating defects of different size and orientation (Fig. 6 left). The first number in every line indicates the height of the font in millimetres. Moving the line sensor over this reference sheet we will get its "eyesight test".

Fig. 6: Engraved aluminium sheet as reference (left). The first number in the line indicates the font size in millimetre. Right: array sensor 64 with measuring wheel on the sheet.

When the engraving is turned up (Fig. 7a) the array probe 32 ends up with font size 5. The Fig. 7b brings up the performance when "looking" through a sound 1-mm-aluminium sheet on the engraving. The signal-to-noise-ratio is lower but big enough for reading the font down to size 7. The Fig. 7c and 7d display the readability with turned down engraving. The largest underlying is reached in Fig. 7d with an additional coverage of a sound 1-mm-sheet. Here, the signal-to-noise ratio is reduced significantly but the size 7 may be read anyway.

Summarizing this investigation, all parts of the letters and signs can be read independently of their orientation despite the anisotropy of the probe elements of the array.
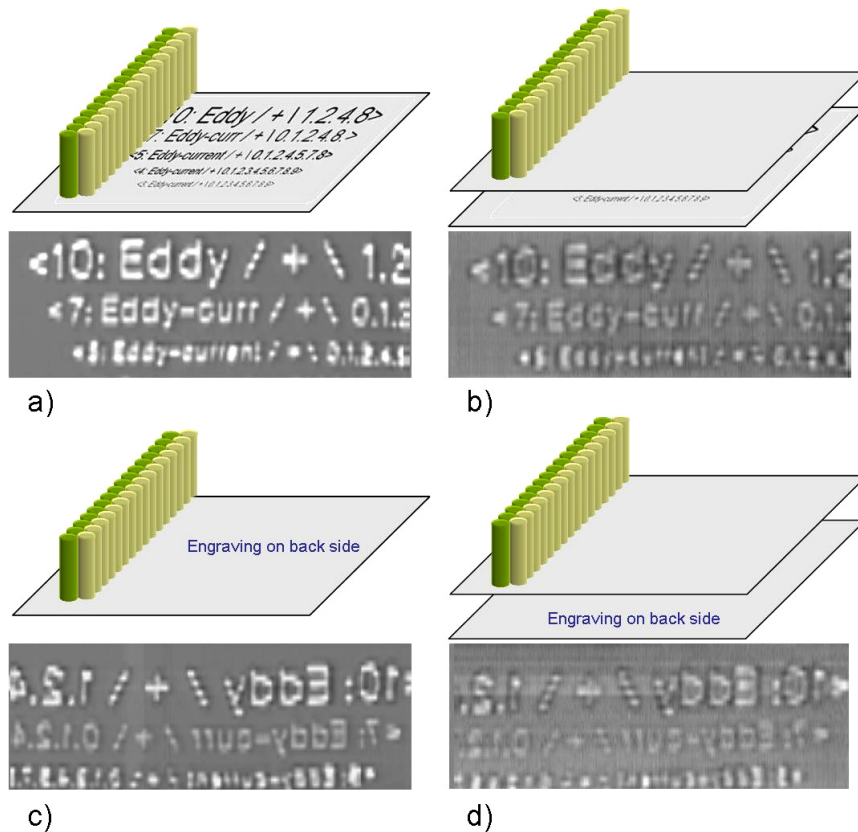

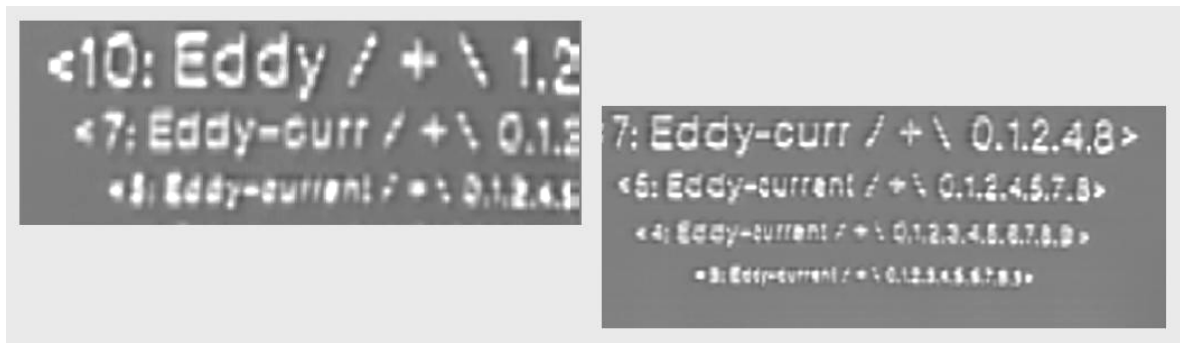Fig. 7: Eyesight test of the probe array 32

Fig. 8: Comparison of spatial resolution of the probe arrays 32 (left) and 64 (right)

Fig. 8 compares the spatial resolution of the probe arrays 32 and 64. With the array 64 alls letters of the smallest font size 4 can be read.

4 Curved sensor lines

For curved surfaces eddy current arrays also may be fitted. Fig. 9 gives some ideas for convex objects like pipes, rods or rails.
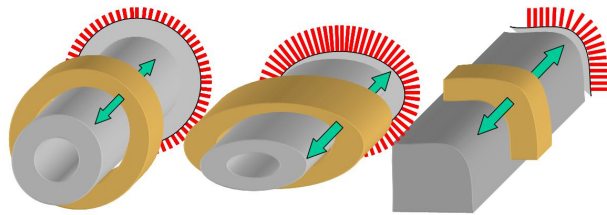

Fig. 9: Potential applications of probe arrays for curved surfaces

The arrays are also suited for concave objects like tube inspection from the inner surface. Fig. 10 displays a probe for 21 mm inner diameter tubes.

USB connector   Housing of 4-channel EC electronics   4 parallel working arrays   centering
and centering

Fig. 10: Low frequency tube inspection probe with four sensor arrays

Four spring-loaded heads cover the complete circumference. Additional sensors record the wall thickness. The inspection speed reaches up to 120 mm/s. The probe contains all analog and digital hardware for the arrays and is connected to a notebook by an extended USB cable of up to 30 m length. No additional power supply is required making the handling most comfortable.

Fig. 11 shows one of the head and its measurement in the complex plane. All sensor signals may be watched simultaneously either in the complex plane or in the C-Scan display. If necessary each sensor may be adjusted individually. The head carrier is made from titanium for minimal wear out. Flexible strips connect each head to its electronics.
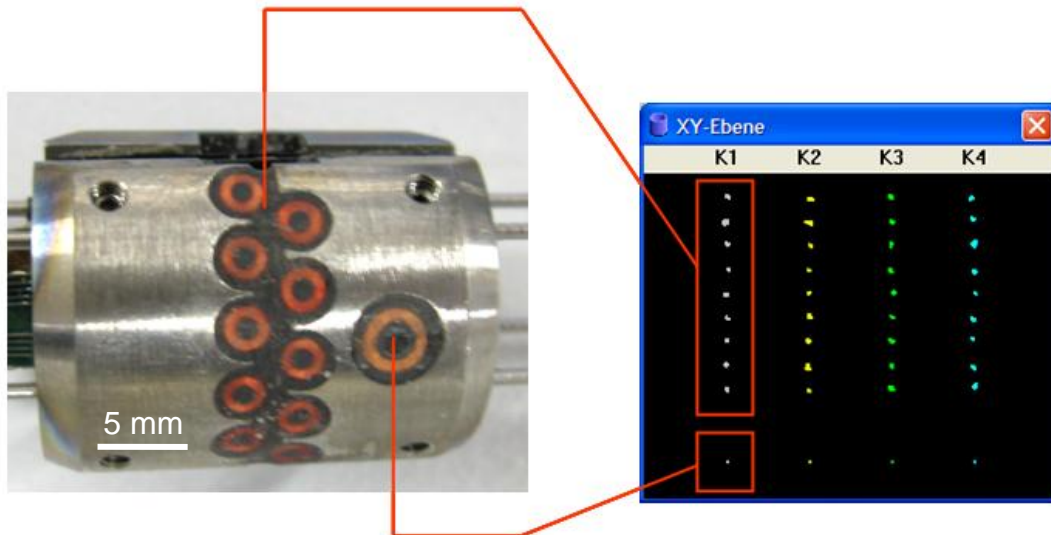
Fig. 11: Single sensor head with coil array and complex plane indication

The C-Scans are recorded from the x- and the y-components of all sensors. The travel distance is recorded by a cable driven wheel encoder. The encoder itself is also plugged to a USB-port of the notebook.

Fig. 12: Circumferential C-Scan image of an austenitic steel tube of 21 mm inner diameter with standard calibration defects of different distance. The scan consists of 36 sensor tracks, scan length about 600 mm.

Fig. 12 displays a 600 mm section of an austenitic steel tube of 21 mm inner diameter. Groups of standard calibration defects become visible differing in their distance.

5   Flat arrays

The principle of multiplexed coils may be extended to 2D-arrays. The first array in Fig. 12 is optimized for large inspection areas covering 38 x 44 mm with a resolution of about 1.5 mm. The array electronics contains the 256-channel eddy current instrument and communicates with a Windows-Notebook via USB. The sensors may work in two different modes. In half-transmission mode each coil corresponds with its neighbours (705 sensors), in single core mode each coil works separately (256 sensors). The build-up time is 0.64 seconds providing an image refresh rate of 1.56 Hz.
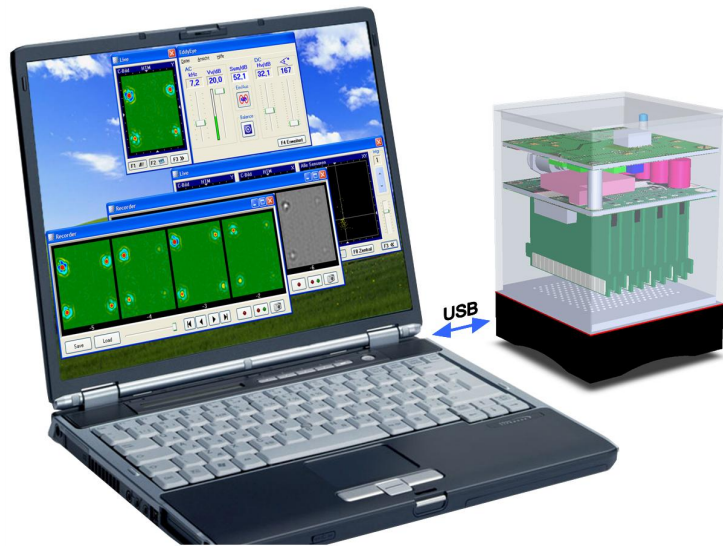
Fig. 13: Flat array consisting of 16x16 coils working as 961 sensors covering an area of
38 x 44 mm. Dimension of the array housing: W x D x H = 60 x 60 x 82 mm.

A second array was optimized for spatial resolution and fast image refreshing. It consists of 60 coils of 2 mm diameter providing a resolution of about 1 mm. The refresh rate reaches the European video clock of 25 Hz.

For increasing the signal-to-noise-ratio the software can integrate over a selectable number of subsequent images. The images may be stored for quality documentation or defect growth analysis. Basing on the magnitude and the angle of the defect signal in the complex measurement plane defect classification becomes possible.

6   Micro-Scanning

When put on the engraved aluminium sheet (Fig. 14) the large array provides images shown in the four right frames of Fig. 15. The individual sensors can be recognized in the image. Only the 10-mm-font and partially the 7-mm-font can be read.
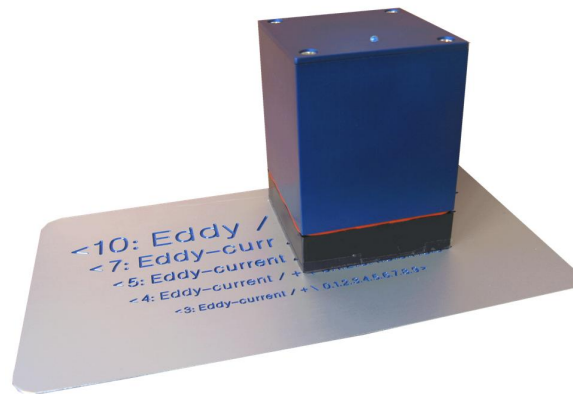

Fig. 14: The flat array on the engraved aluminium sheet for testing the spatial resolution

The idea of micro-scanning [23] consists of moving the array by steps, much lower than the distance between the single sensors and accumulate a weighted resultant image. When moved by 0.5 mm steps the resultant image is much clearer and less noisy than every of the original images. The right frame in Fig. 15 gives the evidence of the increase in readability down to the 5-mm-font. The dark halo of every sign is the result of the Mexican hat PSF.
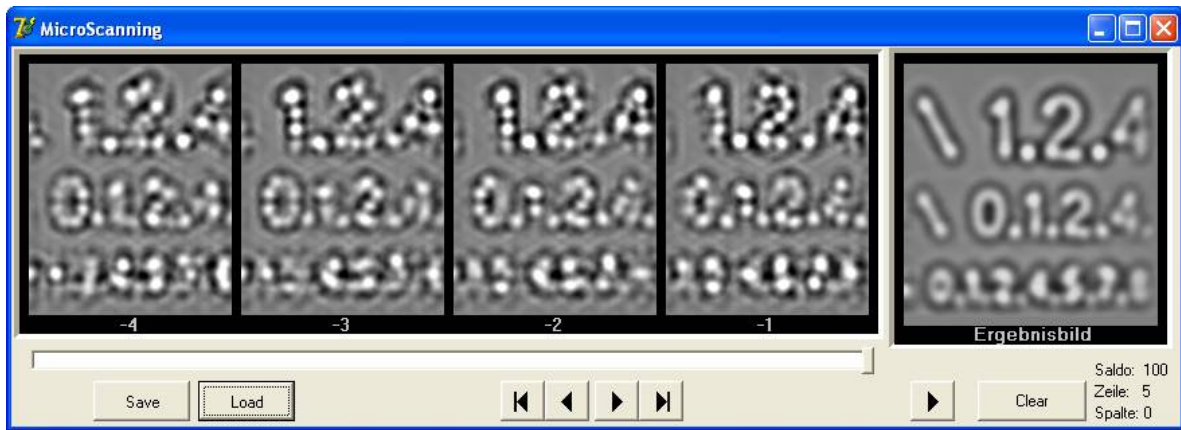
Fig. 15: Images of the flat array in pitch-catch mode on the engraved aluminium sheet.
Left: Sequence of 4 eddy current images gathered with minimal shift of the array by 0.5 mm.
Right: Weighted images following the principles of micro-scanning.

For this micro-scanning the displacement of the array should be measured. Among the possible solutions we find mechanical systems like wheels or optical systems like sensors known from computer mice. These sensors calculate the displacement using two or more subsequent images of the substrate. Known techniques like differential image processing and 2D-correlation algorithms are implemented in a special processor inside the mouse. This method requires a difference in the treated images.

This principle of relative displacement measurement also can be accomplished by the eddy current probe array. Again, a structured area of inspection is needed. This "structure" may be provided even by defects. The array visualizes the movement of the defect and calculates the displacement of the array in x- and y-coordinates. When the object is free from defects or any other structure seen by eddy current method, the displacement cannot be picked up.

For some applications this restriction can be accepted. If only defect documentation is needed, the position of the array is not required. For complete visualization of the inspection area the position of the array always should be known. For this application the array is equipped with a laser mouse sensor nearly working on all surfaces. Fig. 16 explains how an array can fill the whole area of inspection without any gaps.
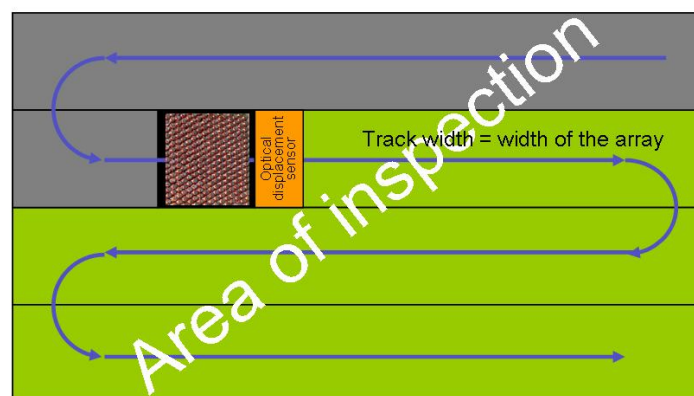

Fig. 16: Covering the area of inspection by a probe array track by track. An optical mouse sensor records the relative position of the array and helps to stitch the track images.

The micro-scanning has another advantage even in this situation. When scanning large areas the array may be moved fast. If there is any indication the sensor is moved slower and the image quality

automatically will enhance for good visualization and documentation. This way, an optimum between inspection speed and image quality is found.

Conclusion

The moving electromagnetic field sensor visualizes open and hidden defects saving all advantages of eddy current inspection. Compared with single probe scanners the handling becomes much easier and cheaper. The eddy current hardware is reduced to a minimum and addresses most signal treatment to the software. This way, the complete electronics is enclosed in the array's housing and easily is connected to the notebook via USB-wire.

Acknowledgements

References

[1] Scholz, A.: Sondenmatte - neuer Weg für die Oberflächenprüfung mit Wirbelstrom. Proc. DGZfP Annl. Conf. Trier May 1990. pp. 218-22.

[2] Grimberg, R.; Savin, A.; Leitoiu, S.; Bruma, A.; Steigmann, R.; Udpa, L.; Udpa, S.: Automated Eddy Current Data Analysis. 4th International Conference on NDT, Hellenic Society for NDT, Chania, Crete-Greece, 11-14 October 2007

[3] Pelletier, E.; Grenier, M.; Chahbaz, A.; Bourgelas, T.: Array Eddy Current for Fatigue Crack Detection of Aircraft Skin Structures. Proc. Vth International Workshop, Advances in Signal Processing for Non Destructive Evaluation of Materials. Québec City (Canada), 2-4 Aug. 2005

[4] Sollier, T.; Talvard, M.; Aïd, M.: Use of EC Sensor Arrays on Thin Films. Electromagnetic Nondestructive Evaluation (IV), S.S. Upda et al. (Eds.), IOS Press, 2000

[5] Yashan, A.; Bisle, W.; Meier, Th.: Inspection of Hidden Defects in Metal-Metal Joints of Aircraft Structures Using Eddy Current Technique with GMR Sensor Array. Proc. 9th ECNDT, Berlin, 2006, paper Tu.4.4.4

[6] Vacher, F.; Gilles-Pascaud, C.; Decitre, J.M.; Fermon, C.; Pannetier, M.; Cattiaux, G.: Non Destructive Testing with GMR Magnetic Sensor Arrays. Proc. 9th ECNDT, Berlin, 2006, paper Tu.4.4.2

[7] Gramz, M.; Stepinski,T.: Eddy Current Imaging array sensors and flaw reconstruction. Research in Nondestructive Evaluation, 5, (1994), pp. 157 -174

[8] Gilles-Pascaud, C.; Lorecki B.; Pierantoni, M.: Eddy current array probe development for non-destructive testing. 16th World Conference on NDT, Montreal, Canada Aug 30 - Sep 3, 2004

[9] Joubert, P.-Y.; Le Diraison, Y.; Pinassaud, J.; Satie, L.: Eddy Current Imager for the Detection of Buried Flaws in Large Metallic Structures. Proc. 9th ECNDT, Berlin, 2006, paper Tu.3.6.1

[10] Perez, L.; Dolabdjian, C.; Waché, C.W.; Butin, L.: Advance in magnetoresistance magnetometer performances applied in eddy current sensor arrays. 16th World Conference on NDT, Montreal, Canada, Aug 30 - Sep 3, 2004

[11] Decitre, J.-M.; Premel, D.; Mangenet, G.; Juliac, E.; Feist, W.D.: Flexible EC Array Probe for the Inspection of Complex Parts developed within the European VERDICT Project. Proc. 9th ECNDT, Berlin, 2006, paper Tu.4.4.3

[12] Gilles-Pascaud C.; Lorecki B.; Pierantoni M.: Eddy Current Array Probe Development for Nondestructive Testing. 16th World Conference on NDT, Montreal, Canada, Aug 30 - Sep 3, 2004

[13] Meilland, P.: Novel Multiplexed Eddy-Current Array for Surface Crack Detection on Rough Steel Surface. Proc. 9th ECNDT, Berlin, 2006, paper Tu.4.8.1

[14] Sullivan, S.P.; Cecco, V.S.; Obrutsky, L.S.; Lakhan, J.R.; Park, A.H.: Validating Eddy Current Array Probes for Inspecting Steam Generator Tubes. ndt.net 1998 January, Vol.3 No.1

[15] Zilberstein, V.; Goldfine, N.; Washabaugh, A.; Weiss V.; Grundy, D.: The use of fatigue monitoring MWM-arrays in production of NDI-Standards with real fatigue cracks for reliability studies. 16th World Conference on NDT, Montreal, Canada, Aug 30 - Sep 3, 2004

[16] Lafontaine, G.; Samson, R.: Eddy Current Array Probes for Faster, Better and Cheaper Inspections. ndt.net, October 2000, Vol. 5 No. 10

[17] Mook, G.; Michel, F.; Simonin, J.; Krüger, M.; Luther, M.: Subsurface Imaging using Moving Electromagnetic Fields and Surface Acoustic Waves. 4th International Conference in Non-Destructive Testing, Stuttgart, Germany, April 2-4, 2007

[18] Mook, G.; Michel, F.; Simonin, J.; Krüger, M.; Luther, M.: Visualization of Hidden Anomalies. 2nd Dresden Airport Seminar: Reliability, Testing, Monitoring of Aerospace Components. Airport Dresden, 15. November 2006

[19] Mook, G.; Michel, F.; Simonin, J.: Wirbelstrom-Bewegtfeldsensoren - Potenziale für die industrielle Anwendung. ZfP in Forschung, Entwicklung und Anwendung, DACH-Jahrestagung, St. Gallen, 28.-30.4.2008, Mo.3.B.1

[20] Mook, G.; Michel, F.; Simonin, J.: Electromagnetic imaging using probe arrays. 17th World Conference on Non-destructive Testing, paper 380, Shanghai, Oct. 25-28, 2008

[21] Reimche, W. et al.: Development and Qualification of a Process-Oriented Nondestructive Test Method for Weld Joints to Operate with Remote Field Eddy Current Technique. Proc. 9th ECNDT, Berlin, 2006, paper Fr.1.7.2

[22] Mook, G.; Hesse, O.; Uchanin, V.: Deep Penetrating Eddy Currents and Probes. 9. ECNDT, Berlin, 25.-29.9.2006, paper 176

[23] Mook, G.; Michel, F.; Simonin, J.: Bildgebende Verfahren zur Prüfung auf oberflächennahe Fehler mittels Wirbelstrom-Sensorarrays, ZfP in Forschung, Entwicklung und Anwendung, DGZfP-Jahrestagung, Münster, 18.-20.5.2009, Berichtsband 115-CD, Mo.3.B.1